Ionization energy of atoms obtained from GW self-energy or from random phase approximation total energies

Fabien Bruneval

Citation: The Journal of Chemical Physics **136**, 194107 (2012);
View online: https://doi.org/10.1063/1.4718428
View Table of Contents: http://aip.scitation.org/toc/jcp/136/19
Published by the American Institute of Physics

Ionization energy of atoms obtained from *GW* self-energy or from random phase approximation total energies

Fabien Bruneval
CEA, DEN, Service de Recherches de Métallurgie Physique, F-91191 Gif-sur-Yvette, France

(Received 1 March 2012; accepted 1 May 2012; published online 17 May 2012)

A systematic evaluation of the ionization energy within the *GW* approximation is carried out for the first row atoms, from H to Ar. We describe a Gaussian basis implementation of the *GW* approximation, which does not resort to any further technical approximation, besides the choice of the basis set for the electronic wavefunctions. Different approaches to the *GW* approximation have been implemented and tested, for example, the standard perturbative approach based on a prior mean-field calculation (Hartree-Fock *GW*@HF or density-functional theory *GW*@DFT) or the recently developed quasiparticle self-consistent method (QS*GW*). The highest occupied molecular orbital energies of atoms obtained from both *GW*@HF and QS*GW* are in excellent agreement with the experimental ionization energy. The lowest unoccupied molecular orbital energies of the singly charged cation yield a noticeably worse estimate of the ionization energy. The best agreement with respect to experiment is obtained from the total energy differences within the random phase approximation functional, which is the total energy corresponding to the *GW* self-energy. We conclude with a discussion about the slight concave behavior upon number electron change of the *GW* approximation and its consequences upon the quality of the orbital energies. © *2012 American Institute of Physics*. [http://dx.doi.org/10.1063/1.4718428]

I. INTRODUCTION

The Green's function approach to many-body problem has been extremely successful for the electronic structure in condensed matter physics. Most noticeably, the *GW* approximation[1] is known to outperform the local and semi-local approximations of density functional theory (DFT) for the description of band gaps and band structures.[2–4] For atoms and molecules, the performance of the *GW* approximation has been studied very little. The seminal results of Shirley and Martin[5] were rather promising, but have had follow-ups only recently.[6–10] However, no systematic study is available yet. Especially the *GW* calculations for open-shell and spin polarized atoms do not exist to the best of our knowledge.

There is no stringent need for accurate orbital energies for atoms, since the ionization energy I for instance can be obtained thanks to a total energy difference

$$I = E_0^{N-1} - E_0^N, \tag{1}$$

where E_0^N stands for the total energy for the N electron system. This is the so-called ΔSCF procedure that produces in general good quality ionization energies at the expense of two separate self-consistent calculations.

In DFT or in many-body perturbation theory, the ionization energy can also be evaluated from the eigenvalues. Within DFT, they are named Kohn-Sham eigenvalues, whereas within many-body perturbation theory, they are called quasiparticle energies. Hence, the ionization energy could alternatively be obtained from the Kohn-Sham or quasiparticle energy corresponding to the highest occupied molecular orbital (HOMO) $\epsilon_{\rm HOMO}^N$ or from the Kohn-Sham or quasiparticle energy corresponding to the lowest unoccupied molecular orbital (LUMO) energy of the $N-1$ electron system $\epsilon_{\rm LUMO}^{N-1}$,

$$I = -\epsilon_{\rm HOMO}^N = -\epsilon_{\rm LUMO}^{N-1}. \tag{2}$$

Generally speaking, the calculation of the ionization energy through the orbital energies yields rather poor results. This problem is not much acute for atoms, as the ΔSCF technique can be used. Nevertheless, it has been understood recently that the poor quality of the potentials (or orbital energies) has also deep consequences on the total energies.[11] The orbital energies are related to the fractional electron behavior, which in turn is related to a localization or delocalization of the wavefunctions. There is therefore a strong need to investigate higher levels of approximation for the potentials.

The *GW* approximation is a successful approximation for self-energies, which, with the Hartree potential, is the effective one-electron potential of a many-electron system. Unfortunately, the *GW* implementation is not unique in practice. Owing to the complexity of the calculations, several types of *GW* calculations have been designed in the last 50 years. The standard approach is not self-consistent and makes use of a prior mean-field calculation as a starting point: this is the so-called G_0W_0 procedure. This situation introduces a dependence of the *GW* result onto the underlying mean-field choice. For solids, the chosen mean-field is very often the local density approximation (LDA) or the generalized gradient approximation (GGA). For atoms and molecules, the starting mean-field happens to be Hartree-Fock (HF) or any other approximation of DFT. The choice of the starting point is unfortunately crucial, since the final *GW* result can be affected by deficiencies in the starting point.[12–15]

In order to get rid of the starting point dependence, self-consistent *GW* would appear appealing at first sight. However, according to the few studies available, the performance of such an approach for the quasiparticle energies is unclear.[7,8,10,16–18] For spectral properties, such as ionization energy, the full self-consistency has been shown to yield incorrect results for the homogeneous electron gas.[16] As far as finite systems are considered, the comprehensive study of 30 molecules by Rostgaard and co-workers[8] shows little or no improvement due to the fully self-consistent *GW* approach. Approximate static self-consistent schemes are then an interesting option;[19,20] they allow one to completely forget about the starting point and they are not affected by the dynamical caveats of the full self-consistency. The quasiparticle self-consistent *GW* (QS*GW*) approach of Faleev and co-workers[19] has been extremely successful for band gaps of solids.[21,22] Besides one single study on molecules,[10] its performance for atoms is however still to be determined.

The purpose of the paper is to evaluate the performance of the *GW* approximation for the ionization energy of the first row atoms. In order to calculate unambiguously converged results, we first present a novel implementation of the *GW* approximation for atoms that are free of the usual drawbacks of standard implementations. Our implementation uses Gaussian basis and does not rely on any further approximation besides the initial choice of the basis set for the wavefunctions. Second, we assess the so far unknown performance of QS*GW* approach for atoms and conclude it yields a small but noticeable improvement over *GW*@HF. Third, we compare three different methods to evaluate the ionization energy of atoms within *GW*: HOMO energy of the atom $-\epsilon^{N}_{\mathrm{HOMO}}$, LUMO energy of the cation $-\epsilon^{N-1}_{\mathrm{LUMO}}$, or total energy difference of the atom and the cation (ΔSCF procedure). The most accurate results for the ionization energy are obtained from ΔSCF and from the HOMO energy. The LUMO energies of the cations yield noticeably worse estimates. We conclude our study with a discussion about the slightly concave upon electron number changes behavior of the *GW* approximation that rationalizes the discrepancy between the three different paths towards the ionization energy.

II. A SHORT REVIEW OF THE *GW* APPROXIMATION

A. General theory

The *GW* self-energy arises from the many-body perturbation theory, when the considered perturbation is not in the bare Coulomb interaction $v(\mathbf{r},\mathbf{r}') = 1/|\mathbf{r}-\mathbf{r}'|$ (in atomic units), but is in the screened Coulomb interaction W. The effective interaction W accounts for the screening of the interactions by the electrons of the system. W is anticipated to be smaller and better behaved than v. Most importantly, the long-ranged part is damped out for metallic systems or reduced for the other systems. The *GW* self-energy may be thought of as a dynamically screened generalization of the Fock exchange.

In practice, the *GW* self-energy is built from the frequency convolution of the Green's function G with the screened Coulomb interaction W,

$$\Sigma^{GW}(\mathbf{r},\mathbf{r}',\omega) = \frac{i}{2\pi}\int d\omega' e^{i\eta\omega'} G(\mathbf{r},\mathbf{r}',\omega+\omega') \times W(\mathbf{r}',\mathbf{r},\omega'), \quad (3)$$

where η is a vanishing positive real number.

Introducing the polarizable part of the screened Coulomb interaction $W_p = W - v$, the self-energy can be conveniently split in the usual Fock exchange operator

$$\Sigma_x(\mathbf{r},\mathbf{r}') = \frac{i}{2\pi} v(\mathbf{r},\mathbf{r}') \int d\omega' e^{i\eta\omega'} G(\mathbf{r},\mathbf{r}',\omega') \quad (4)$$

and a remainder Σ_c^{GW}. By definition, the remainder accounts for the correlation effects. The term $e^{i\eta\omega'}$ in Eq. (4) retains only the contribution from the occupied states in the Green's function.

The polarizable part of the screened Coulomb interaction W_p is in turn a function of the random phase approximation (RPA) polarizability χ of the electronic system,

$$W_p(\mathbf{r},\mathbf{r}',\omega) = \int d\mathbf{r}_1 d\mathbf{r}_2 v(\mathbf{r},\mathbf{r}_1)\chi(\mathbf{r}_1,\mathbf{r}_2,\omega)v(\mathbf{r}_2,\mathbf{r}'). \quad (5)$$

Then the RPA polarizability χ can be related to the independent particle polarizability χ_0 through a Dyson-like equation,

$$\chi^{-1}(\mathbf{r},\mathbf{r}',\omega) = \chi_0^{-1}(\mathbf{r},\mathbf{r}',\omega) - v(\mathbf{r},\mathbf{r}') \quad (6)$$

that connects the non-interacting system to the interacting system. Finally, χ_0 has a simple expression in terms of two Green's functions,

$$\chi_0(\mathbf{r},\mathbf{r}',\omega) = -i\int d\omega' G(\mathbf{r},\mathbf{r}',\omega+\omega')G(\mathbf{r}',\mathbf{r},\omega'). \quad (7)$$

Using the diagrammatic language, χ_0 is a ring diagram and the RPA polarizability χ is the infinite sum over the ring diagrams. Symbolically, it reads

$$\chi = \chi_0 + \chi_0 v \chi_0 + \chi_0 v \chi_0 v \chi_0 + \dots . \quad (8)$$

The *GW* diagrams for the correlation self-energy are displayed in panel (b) of Fig. 1. It contains an infinite summation over all the ring diagrams. The second-order approximation (or MP2 when the Green's functions are HF ones[23]), on the other hand, not only contains the first of the ring diagrams, but also includes the second-order exchange diagram (panel (a)).

B. The perturbative *GW* approach

In principle, the Green's function appearing in Eqs. (3) and (7) should be obtained self-consistently from the iteration of the Dyson equation. In reality, this is hardly feasible and may be not desirable[7,8,16–18] as discussed in the Introduction. It is then common practice[1–3] to consider the Green's function from another simpler approximation: LDA, GGA, HF, etc. We denote these approaches as *GW*@LDA, *GW*@GGA, *GW*@HF, respectively.

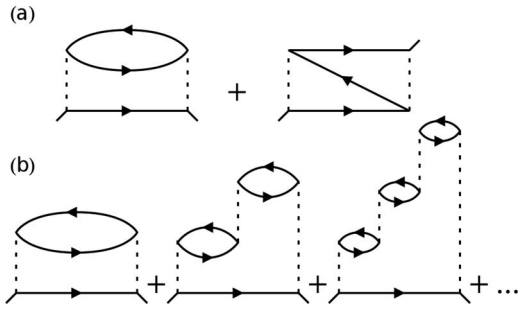

FIG. 1. Correlation self-energy diagrams included in the second-order approximation [panel (a)] and in the *GW* approximation [panel (b)]. The solid lines with arrows represent the one-particle Green's function G and the dashed lines represent the Coulomb interaction v. The second-order self-energy consists of the one-ring diagram and of the second-order exchange, whereas the *GW* self-energy contains the infinite sum over the ring diagrams. If the Green's functions are HF Green's functions, the second-order self-energy is named MP2.

Within a mean-field approach with eigenvalues $\epsilon_{i\sigma}$ and eigenvectors $\varphi_{i\sigma}(\mathbf{r})$, the Green's function simply reads

$$G(\mathbf{r},\mathbf{r}',\omega) = \sum_{i\sigma} \varphi_{i\sigma}(\mathbf{r})\varphi_{i\sigma}(\mathbf{r}') \times \left[\frac{f_{i\sigma}}{\omega - \epsilon_{i\sigma} - i\eta} + \frac{1-f_{i\sigma}}{\omega - \epsilon_{i\sigma} + i\eta} \right], \quad (9)$$

where the wavefunctions have been assumed to be real and $f_{i\sigma}$ is the occupation number of state i with spin σ. The Green's function depends on all the orbitals: occupied and virtual. Its poles are the eigenvalues, slightly shifted above or below the real axis.

With this definition for the Green's function, the equations presented in Sec. II A can be tracted numerically and finally, the *GW* quasiparticle energy reads

$$\epsilon_{i\sigma}^{GW} = \epsilon_{i\sigma}^{\mathrm{HF}} + \left\langle i\sigma \middle| \Sigma_c^{GW}(\epsilon_{i\sigma}^{GW}) \middle| i\sigma \right\rangle. \quad (10)$$

Please note that the self-energy is a dynamical operator and needs to be evaluated precisely at the unknown quasiparticle energy. This is not an issue since the equation can be solved for instance graphically as exemplified in Fig. 2.

C. Quasiparticle self-consistent *GW*

The dependence of the *GW* result onto the starting mean-field Green's function is not elegant in theory and can introduce additional issues in practice. It would be desirable to perform the calculations self-consistently, so that the starting point is forgotten.

Recently, the quasiparticle self-consistent *GW* (QS*GW*) was introduced by Faleev and co-workers[19] in order to get a simplified version of self-consistent *GW* calculations. They proposed a static and hermitian approximation to the *GW* self-energy,

$$\left\langle i\sigma \middle| \Sigma_c^{\mathrm{QS}GW} \middle| j\sigma \right\rangle = \frac{1}{2}\left[\left\langle i\sigma \middle| \Sigma_c^{GW}(\epsilon_{j\sigma}) \middle| j\sigma \right\rangle + \left\langle j\sigma \middle| \Sigma_c^{GW}(\epsilon_{i\sigma}) \middle| i\sigma \right\rangle \right] \quad (11)$$

that conserves the orthogonality of the underlying wavefunctions and the real-valued eigenvalues. The advantage of this particular expression is that only the off-diagonal terms ($i \neq j$) are approximated. Once self-consistency has been reached, the diagonal expectation values of Σ_c are evaluated precisely at the quasiparticle energy, as they should be according to Eq. (10).

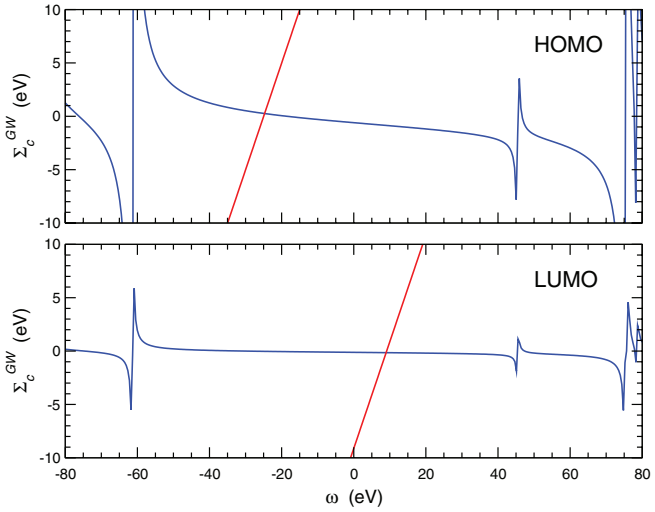

FIG. 2. HOMO (upper panel) and LUMO (lower panel) expectation values of the correlation part of the dynamical *GW* self-energy based on HF inputs (*GW*@HF) for He using a cc-pV5Z basis. The small real number η has been set to 0.25 eV. The crossing point between the straight line and the self-energy is the solution of the quasiparticle equation (10).

D. RPA total energy

Finally, we close the theoretical review by introducing the RPA expression for the total energy. This approximation is tightly bound the *GW* self-energy: the *GW* self-energy operator is obtained from the functional derivative of the RPA functional Φ_c^{RPA} with respect to the Green's function,[24]

$$\Sigma_c^{GW}(\mathbf{r},\mathbf{r}',\omega) = \frac{\delta\Phi_c^{\mathrm{RPA}}}{\delta G(\mathbf{r}',\mathbf{r},-\omega)}, \quad (12)$$

where the RPA functional symbolically reads

$$\Phi_c^{\mathrm{RPA}} = -\frac{1}{2}\mathrm{Tr}\left[\sum_{n=2}^{+\infty} \frac{(v\chi_0)^n}{n} \right]. \quad (13)$$

The symbol Tr is short for the triple integral over $\mathbf{r}$, $\mathbf{r}'$, and ω. More details can be found for instance in Ref. 25. The RPA functional is the infinite sum over the ring diagrams. In summary, the functional Φ_c^{RPA} yields the correlation energy corresponding to the *GW* approximation to the self-energy. The connection between the two frameworks will be numerically investigated in the following.

III. PRACTICAL IMPLEMENTATION

The main target of the present work is to obtain unambiguous values. Therefore, we resort to as few approximations as possible. Basically, all the calculations are exact, once the basis for the wavefunctions has been set. The computational efficiency is clearly not the issue here.

We adopt an all-electron formalism to solve the non-relativistic Schrödinger equation. The self-consistent field equations are solved in the unrestricted manner, for which, the spin-up and spin-down wavefunctions are allowed to differ. The wavefunctions are expanded in a Gaussian basis. Unlike previous implementations in a Gaussian basis,[6,9] we do not resort to any auxiliary basis set to expand the polarizabilities. Furthermore, the RPA polarizability is obtained in the product basis set $|ij\sigma\rangle$, so that its frequency dependence is exactly known and can be integrated analytically.[26] As a consequence, no plasmon-pole model,[3,27] nor analytic continuation[10,28] is needed. In summary, once the basis set has been chosen, there is no other convergence parameter of any kind.

A. The Gaussian basis set

For convenience, we adopt the Cartesian Gaussian basis functions

$$\phi_\alpha(\mathbf{r}) = N x^{n_x} y^{n_y} z^{n_z} e^{-\zeta r^2}, \tag{14}$$

where ζ is the decay rate, $l = n_x + n_y + n_z$ defines the angular momentum of the Gaussian basis function, and N is the normalization factor. The decay rates are obtained from the Dünning's correlation consistent sets[29] as reported in a web-available database.[30,31] Even though the original basis sets from Dünning were defined for pure Gaussian functions with spherical harmonics describing the angular part, the use of Cartesian Gaussian just adds a few basis functions and affects the final result very little. For instance, with Cartesian Gaussians, there are six d orbitals instead of the usual five; there are 10 f orbitals instead of the usual seven; etc. The use of the Dünning sets cc-pVXZ (with X = D, T, Q, 5, or 6) allows us to reduce the basis set error in a systematic manner.

The overlap, the kinetic, the nucleus attraction integrals are readily obtained from basic formulas. The numerical value of the four Gaussian electron repulsion integrals

$$(\alpha\beta|\gamma\delta) = \int d\mathbf{r}_1 d\mathbf{r}_2 \phi_\alpha(\mathbf{r}_1)\phi_\beta(\mathbf{r}_1)\frac{1}{|\mathbf{r}_1 - \mathbf{r}_2|}\phi_\gamma(\mathbf{r}_2)\phi_\delta(\mathbf{r}_2) \tag{15}$$

can be obtained from a web-available library.[32]

The most cumbersome part of a *GW* calculation is the transformation of the electron repulsion integrals into the eigenvector basis,

$$(ij\sigma|kl\sigma') = \sum_{\alpha\beta\gamma\delta} C_{\alpha i\sigma} C_{\beta j\sigma} C_{\gamma k\sigma'} C_{\delta l\sigma'} (\alpha\beta|\gamma\delta), \tag{16}$$

where $C_{\alpha i\sigma}$ are the expansion coefficients of the eigenvectors into the Gaussian basis set. This operation scales as N^5 with N being the number basis functions. The same bottleneck is also encountered in MP2 calculations.

B. RPA equation in the product basis

Once these electron repulsion integrals are available, we are able to evaluate the *GW* approximation for atoms. We first solve the RPA equation in the product basis set $|ab\sigma\rangle$, where a and b are indexes over the mean-field eigenstates. This equation requires the diagonalization of the RPA two-particle Hamiltonian H_{RPA},

$$H_{\mathrm{RPA}\ ab\sigma}^{\ cd\sigma'} = (\epsilon_{b\sigma} - \epsilon_{a\sigma})\delta_{ac}\delta_{bd}\delta_{\sigma\sigma'} + (f_{a\sigma} - f_{b\sigma})(ab\sigma|cd\sigma'). \tag{17}$$

The product basis is limited to occupied-virtual or virtual-occupied pairs. This operation is then a matrix diagonalization of dimension $2N_{\mathrm{occupied}}N_{\mathrm{virtual}}N_{\mathrm{spin}}$. The diagonalization problem is non-symmetric. Let us consider the matrix R containing the right-eigenvectors,

$$H_{\mathrm{RPA}} R = R D. \tag{18}$$

The matrix D stands for the diagonal matrix containing the eigenvalues E_λ. The eigenvalues E_λ represents the neutral excitations with positive energy (resonant part of the spectrum) and negative energy (antiresonant part of the spectrum). The right eigenvectors R_λ are then expanded in the product basis $|ab\sigma\rangle$. The problem could be recast in a symmetric manner using the so-called Casida equations.[33]

Using the eigenvectors and eigenvalues of the RPA Hamiltonian, the polarizability χ can be written in the product basis,

$$\chi_{ab\sigma}^{cd\sigma}(\omega) = \sum_\lambda R_{\lambda ab\sigma}(\tilde{R}^{-1})_{\lambda cd\sigma} \times \left[\frac{\Theta(E_\lambda)}{\omega - E_\lambda + i\eta} + \frac{\Theta(-E_\lambda)}{\omega - E_\lambda - i\eta}\right], \tag{19}$$

where the index λ runs over the solutions of the RPA equation and $\tilde{R}^{-1}$ is a short notation for the matrix inverse of R the columns of which were multiplied by the occupation number difference. The Heavyside function $\Theta(E_\lambda)$ ensures the correct polar structure for a time-ordered response function: the negative energies E_λ are located just above the real axis of the complex plane and the positive energies just below.

C. *GW* self-energy with exact frequency dependence

Hence, introducing the Green's function from Eq. (9) and $W_p = v\chi v$ from Eq. (19) into the correlation self-energy Σ_c^{GW}, the residue theorem allows one to perform exactly the frequency integral. The final expression for *GW* self-energy reads

$$\left\langle i\sigma|\Sigma_c^{GW}(\omega)|j\sigma\right\rangle = \sum_{k\lambda} M_{\lambda ik\sigma}\tilde{M}_{\lambda kj\sigma}\left[\frac{f_{k\sigma}\Theta(E_\lambda)}{\omega - \epsilon_{k\sigma} + E_\lambda - i\eta} - \frac{(1 - f_{k\sigma})\Theta(-E_\lambda)}{\omega - \epsilon_{k\sigma} + E_\lambda + i\eta}\right], \tag{20}$$

where the intermediate matrix products

$$M_{\lambda ik\sigma} = \sum_{ab} R_{\lambda ab\sigma}(ik\sigma|ab\sigma) \tag{21}$$

and

$$\tilde{M}_{\lambda kj\sigma} = \sum_{cd}(\tilde{R}^{-1})_{\lambda cd\sigma}(cd\sigma|kj\sigma) \tag{22}$$

have been introduced. Note that the *GW* self-energy is diagonal in spin.

The polar structure of Σ_c can be observed in Fig. 2. The poles are located $\epsilon_{k\sigma} + E_\lambda$. The self-energy is very weakly

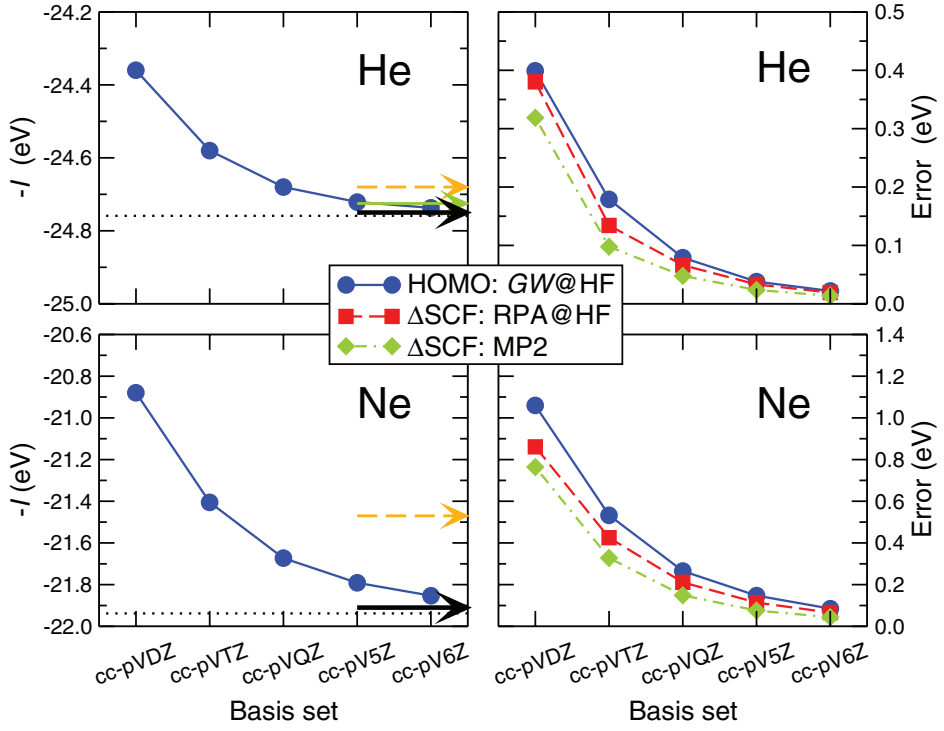

FIG. 3. Basis set convergence of the ionization energy of helium (upper panels) and neon (lower panels). The ionization energy is obtained from the HOMO energy of the atom within *GW*@HF in the left-hand panels. The horizontal arrows show the HOMO energy from literature's calculations in Ref. 6 (dashed arrow), in Ref. 7 (thick arrow), and in Ref. 10 (thin arrow). The horizontal doted line shows the complete-basis set limit using a simple extrapolation scheme.[35] The right-hand panels compare the convergence rates of the HOMO energy within *GW*@HF (circles) to the ΔSCF procedure using RPA@HF (squares) or using MP2 (diamonds).

frequency-dependent in the range of interest, i.e., in the region where the two curves intersect. In other words, the renormalization factor of the quasiparticle peaks is close to 1. The closest poles are approximately at HOMO energy minus the HOMO-LUMO gap and at the LUMO energy plus the HOMO-LUMO gap.

The implementation of QS*GW* is then straightforward. The full matrix $\langle i\sigma|\Sigma_c^{\mathrm{QS}GW}|j\sigma\rangle$ is calculated and then transformed back into the basis representation $\langle\alpha|\Sigma_c^{\mathrm{QS}GW}|\beta\rangle$ for spin up and spin down. The only additional difficulty arises from the self-consistency loop stabilization. We employ here a simple mixing scheme. We mix not only the density matrix, as it is customary for HF calculations, but also the self-energy matrix itself, since the self-energy depends directly onto the energies and the wavefunctions. With a mixing parameter of 0.5, we were able to achieve good convergence even with the largest basis sets of the present work using a maximum of 60 cycles.

D. RPA correlation energy

The RPA correlation energy is obtained as a by-product of the calculation of the polarizability χ. Indeed, Furche showed[34] that the RPA correlation energy can be obtained from the formula,

$$E_c^{\mathrm{RPA}} = \frac{1}{2}\sum_{\substack{\lambda \\ E_\lambda>0}} \left(E_\lambda - E_\lambda^{TDA}\right), \qquad (23)$$

where the sum has been limited to positive excitation energies and the excitation energies E_λ^{TDA} are obtained within the Tamm-Dancoff approximation that ignores the coupling between occupied to virtual excitations and virtual to occupied excitations. In practice, we perform a self-consistent HF (resp. QS*GW*) calculation and calculate the RPA correlation energy out of the HF (resp. QS*GW*) eigenvectors and eigenvalues. We label this procedure RPA@HF (resp. RPA@QS*GW*).

IV. CONVERGENCE AND ACCURACY

Before starting the systematic calculations, let us first check the reliability of the method. We first test the basis set convergence for some selected elements and then check our results against the very few published data for the first row atoms.

The basis set convergence is shown in Fig. 3 for the ionization energy of He and Ne. We observe the slow convergence of the *GW*@HF HOMO energy as a function of the basis set size. For Ne, an accuracy of 0.1 eV is obtained at the expense of a cc-pV5Z basis, which corresponds to 126 Cartesian Gaussian functions and a maximum angular momentum of $l = 5$. The rate of convergence is somewhat slower than reported for molecules in the previous Gaussian *GW* implementations.[6,9,10,36] However, it seems to be consistent with the convergence rate of RPA energies. RPA energies have been observed to require extremely complete basis sets in order to achieve chemical accuracy.[37] Figure 3 also shows the convergence rate of the ionization energy using the difference

TABLE I. Review of the previously published *GW* ionization energies and electron affinities of the first row atoms, and comparison with our results within the cc-pV5Z basis.

	HF+*GW*		LDA+*GW*		QS*GW*		
	This work	Earlier studies	This work	Earlier studies	This work	Earlier studies	Expt.[a]
Ionizations							
H			− 12.85	−12.66[b]			− 13.61
He	− 24.72	−24.68,[c] −24.73,[d] −24.75[e]	− 23.92	−23.65,[e] −24.20[f]			− 24.59
Be	− 9.16	−9.17,[d] −9.19[e]	− 9.02	−8.88,[e] −9.24[f]			− 9.32
B^+	− 24.88	−24.9[g]					− 24.15
Ne	− 21.79	−21.47,[c] −21.91[e]	− 20.97	−21.06,[e] −20.55[f]			− 21.56
Na			− 5.32	−5.40[h]	−5.43	−5.49[h]	− 5.15
Mg	− 7.62	−7.69[e]	− 7.53	−7.52[e]			− 7.65
Al^+	− 18.76	−18.9[g]					− 18.83
Ar	− 16.07	−15.94[c]					− 15.76
Electron affinities							
B^+	− 8.46	−8.5[g]					− 8.30
Na^+			− 4.71	−4.88[h]	−5.06	−5.05[h]	− 5.15
Al^+	− 6.01	−6.0[g]					− 5.99

[a]Reference 39.
[b]Reference 40.
[c]Reference 6.
[d]Reference 10.
[e]Reference 7.
[f]Reference 41.
[g]Reference 5.
[h]Reference 42.

of RPA total energies of the atom and of the positive ion. The convergence rate of the ΔSCF procedure nicely follows the convergence of the *GW* HOMO energy. Such a slow convergence is not surprising for perturbation theory. The MP2 calculations also shown in Fig. 3 are known to slowly converge to the complete basis set limit.[35,38]

From now on, all the calculations will be performed using the Dunning's cc-pV5Z basis set. This kind of basis appears as sufficient to ensure a 0.1 eV accuracy. The number of basis functions ranges from 70 for hydrogen to 130 for argon.

Table I compares our evaluation of *GW*@LDA, at *GW*@HF, and QS*GW* ionization energies and electron affinities with all the available results in the literature we are aware of. Results published to date use different basis sets: Gaussian basis sets for Refs. 6 and 10, numerical radial grid for Refs. 5, 7, 40, and 41 and plane-waves for Ref. 42. The overall agreement of our values with the published values is rather good, especially for *GW*@HF. The somewhat larger discrepancies for *GW*@LDA may possibly be attributed to the generalized Koopmans' theorem employed in Ref. 7. Note that agreement with the oldest results of Shirley and Martin is good.[5] The most similar implementation to ours[10] yields impressively similar results (within 0.01 eV). The only QS*GW* result for an atom from the literature also agrees well with our implementation.[42]

In Secs. V A–V C, we provide accurate evaluation of the ionization energy for all the first row atoms. These atoms include open-shell atoms, which are delicate to treat in a mean-field approach. Some approximations, such as local and semi-local approximations of DFT, minimize the total energy with fractional occupation numbers. Other approximations, such as HF and QS*GW*, do favor integral occupation numbers. In the present study, only approximations of the latter kind have been considered for the open-shell atoms and therefore, the occupation numbers have been safely set to integers.

V. IONIZATION OF ATOMS

A. Magnitude of the screening for atoms

Here, we evaluate the importance of the screening of the interactions for atoms. The perturbation theory in solids is often based on the screened Coulomb interaction W, whereas for atoms, it is rather based on the bare Coulomb interaction v. The rational behind this choice is the weak screening attributed to atoms. Indeed, the electrons in isolated atoms are localized and weakly polarizable. Therefore, it would be pointless using the complex W instead of the simple v for atoms. This explains why the *GW* approximation is prominent for the condensed matter, whereas the Møller-Plesset approximations are in use for gas phase calculations.

We would like to check explicitly the influence of using v or W for atoms. The comparison is exemplified with the HOMO expectation value for different approximations to the correlation self-energy Σ_c. The complete *GW* self-energy is compared to the first term in the ring diagram expansion (see Fig. 1). The one-ring self-energy is contained both in the MP2 approach and in the *GW* approach. The self-energy truncated to one-ring only is easily derived from Eq. (5), where χ is replaced by χ_0.

Figure 4 demonstrates that the difference between the infinite sum of ring diagrams and the truncation to the first

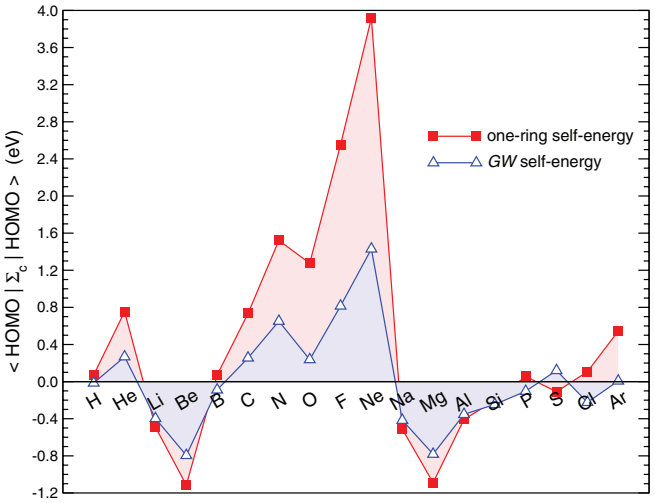

FIG. 4. HOMO expectation value of the correlation self-energy for the one-ring self-energy (squares) and for the *GW* self-energy (open triangles) for the light atoms. The calculations are based on HF inputs in a cc-pV5Z basis set.

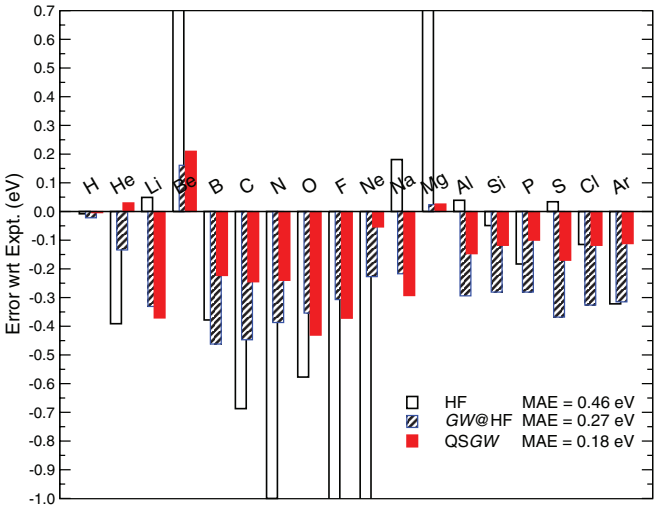

FIG. 5. Deviation from experiment[39] in the HOMO energy $\epsilon^N_{\rm HOMO} - (-I)$ of the light atoms within cc-pV5Z basis set for HF (open bars), *GW*@HF (striped bars), or QS*GW* (solid bars). The mean-absolute error (MAE) is also provided.

diagram is sizable. As expected, the *GW* self-energy is in general smaller than the one-ring counterpart. The statement is clear for the first row atoms and more contrasted for the second row. The closed-shell atoms (He, Be, Ne, Mg, Ne) are especially sensitive to the truncation of the sum over ring diagrams. We conclude that W is a better choice for a perturbation expansion, even for the light atoms.

B. HOMO of atoms and LUMO of cations

As explained in the introduction, there are several ways to evaluate the ionization energy of an atom. Most commonly, the total energy difference in the atom and the singly positively charged ion is taken. Alternative choices are the atom HOMO energy or the cation LUMO energy [Eq. (2)]. Within an exact theory, these three quantities are identical. Within DFT or HF, these three evaluations strongly deviate. There are some early indications *GW* should be much better.[42] We now consider these alternative forms for HF and two kinds of *GW*: *GW*@HF and QS*GW*.

Figure 5 shows the error with respect to experimental negative ionization energy: $\epsilon^N_{HOMO} - (-I)$. It is well known that the HF HOMO energy is not catastrophic in predicting the ionization energy. As might be expected because screening is weak, *GW*@HF and QS*GW* are quite similar. All the *GW* based approaches underestimate the position of the HOMO by a small amount. The perturbative *GW* approach seems to be justified for atoms: even when the HF starting point is noticeably wrong (e.g., for atoms of the end of the first row), the *GW*@HF performs almost as well as QS*GW*. Note that the *GW* correlation contains a small self-interaction: the HOMO of the hydrogen atom is not exact.

In Fig. 6, we provide the error with respect to experiment for the LUMO energy of singly positively charged ions within same three approximations. It is well known from text books that the LUMO in HF gives a very poor estimate to the ionization energy. We calculated a huge mean-absolute error (MAE) of 1.74 eV. The different *GW* flavors, *GW*@HF and QS*GW*, once again perform rather well in predicting the correct position of the cation LUMO energy. The MAE error is twice larger than for the positioning of the HOMO of atoms. Generally speaking, the self-consistency improves over the perturbative *GW*@HF for cations, except for carbon and silicon. When the HF starting point is completely off, the self-consistency can help much sometimes, as can be observed for the atoms of the end of the first row series and sometimes does not do much, as for the end of the second row series. In general, the *GW* based methods slightly overestimate the position of the LUMO of singly positively charged ions.

In order to reach the best agreement with experiment, it appears safer so far to evaluate the ionization energy with the *GW* approximation from the HOMO of the atom rather than from the LUMO of cations.

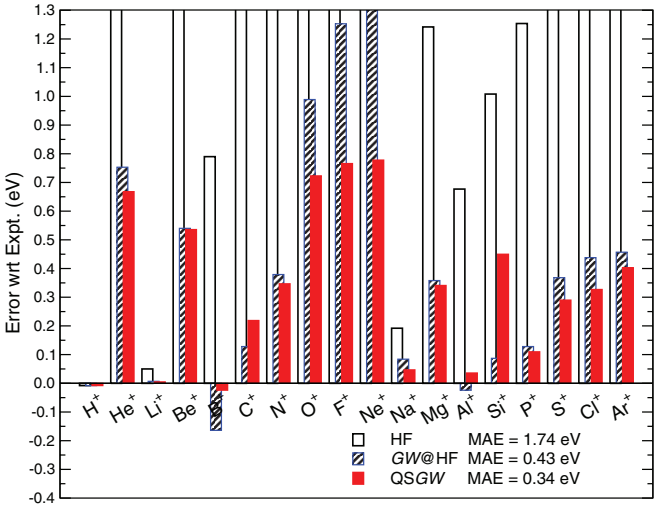

FIG. 6. Deviation from experiment[39] in the LUMO energy $\epsilon^{N-1}_{\rm LUMO} - (-I)$ of the light singly positively charged ions within cc-pV5Z basis set for HF (open bars), *GW*@HF (striped bars), or QS*GW* (solid bars). The mean-absolute error (MAE) is also provided.

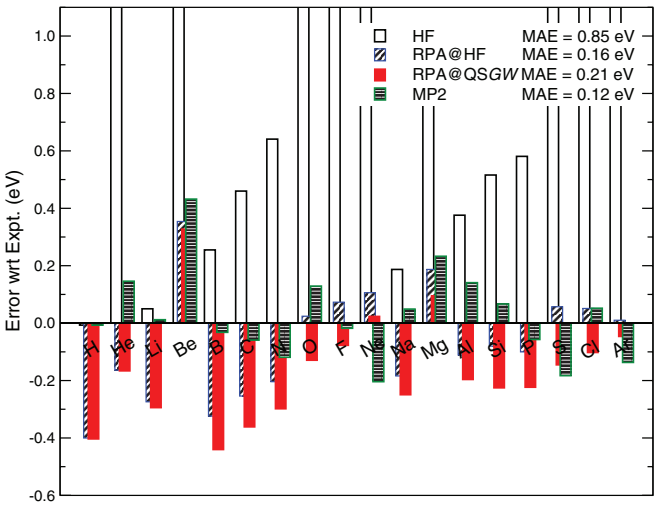

FIG. 7. Deviation from experiment[39] using the ΔSCF procedure $E_0^N - E_0^{N-1} - (-I)$ within cc-pV5Z basis set. Different levels of theory are shown: HF (open bars), RPA@HF (oblique striped bars), RPA@QS*GW* (full bars), MP2 (horizontally striped bars). The mean-absolute error (MAE) is also provided.

C. ΔSCF evaluation of the ionization energy

We now turn to the classical method to evaluate the ionization energy of atoms, namely the ΔSCF procedure. Figure 7 shows the error in calculating the ionization energy from the total energy difference described in Eq. (1). The RPA expression for the correlation energy corresponds to the *GW* approximation for the correlation self-energy. RPA energy and *GW* self-energy are, in principle, closely related. We hence employed four different approximations for the total energies: HF, RPA based on HF inputs, RPA based on QS*GW* inputs, and the standard MP2 approximation. For the ΔSCF procedure, MP2 clearly prevails over the other approximations. The second-order exchange diagram, as drawn in Fig. 1, which is present in MP2 and absent in RPA, is undoubtedly important for atoms. Thanks to this diagram, MP2 is devoid of self-interaction, whereas RPA suffers from self-interaction to some extent. This is clearly seen in the case of the hydrogen atom.

In the present work, we do not evaluate the RPA energy self-consistently with the corresponding RPA potential. However, the RPA functional is a stationary expression for the total energy. And even though the stationarity is believed to be limited,[25] the results should be weakly sensitive to the input Green's function. This is indeed what we observe in Fig. 7: RPA@HF and RPA@QS*GW* are in overall agreement. Surprisingly, RPA@HF appears slightly better than RPA@QS*GW* even when the HF starting point is clearly wrong. This statement calls for further investigations.

VI. CONCAVITY OF THE *GW* APPROXIMATION

How a particular approximation varies with fractional occupation number offers insight into its qualities and limitations. In the exact theory, the total energy should be a straight line in between the integral number of electrons.[43,44] Thus, the derivative of the energy with respect to electron number should be constant in between two consecutive integers and equal to the total energy difference. This last quantity is nothing else but the orbital energy (including a possible exchange-correlation discontinuity in the case of local Kohn-Sham potentials).[45,46]

In practice, the exchange-correlation approximations never induce the perfect straight line behavior. The deviation from the straight line is a sign of a localization or delocalization error.[11,47] In general, the approximations to DFT yield a convex total energy and therefore suffer from a delocalization error. An electron added to a system made of two identical well-separated subsystems minimizes its energy by splitting: half an electron goes on each subsystem. On the other hand, the HF approximation induces a concave total energy and is therefore affected by a localization error. The aforementioned extra electron lowers its energy by localizing on one single subsystem. In the exact theory, spreading or localizing the electron should not affect the total energy.

In Ref. 42, we established that for clusters in Na and certain defects in SiC, localized energy levels were slightly concave with respect to occupation. The concavity can be accessed from the ordering between the LUMO energy of a positive ion and the HOMO energy of the corresponding atom, if one assumes a monotonic behavior of the orbital energy as a function of the fractional number of electrons. This is generally the case, except for MP2 to a small extent.[48]

In Fig. 8, we recast the previously calculated orbital energies now considering ΔSCF as the reference. From the upper panel, one can observe that the HF approximation is clearly concave. Indeed, the HOMO energy of the atom is always much lower than the total energy difference, whereas the LUMO energy of the positive ion is always much higher. The atom HOMO energy, nor the cation LUMO energy, are a good estimate for the total energy difference. The deviation is very large in both cases. Following Slater's argument,[49]

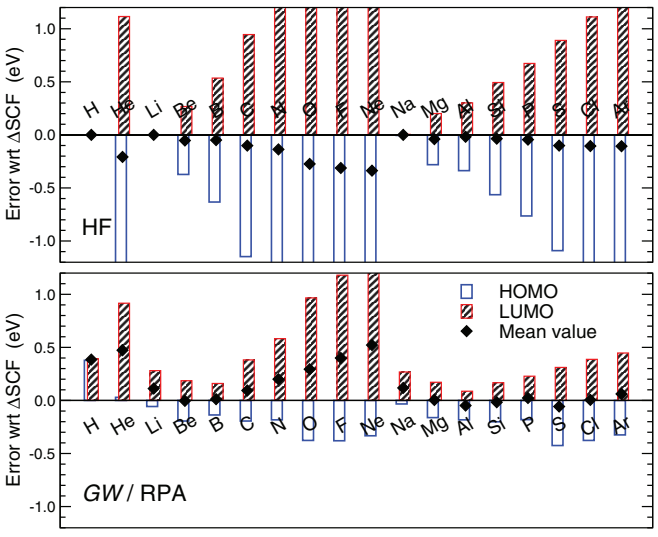

FIG. 8. Deviation from ΔSCF reference for the atom HOMO energy $\epsilon^N_{\rm HOMO}$ (open bars) and of the cation LUMO energy (striped bars). The mean value of the HOMO and the LUMO is displayed with the diamond symbol. The upper panel compares HF orbital energies to the HF total energy difference. The lower panel compares *GW*@HF orbital energies to the RPA@HF total energy difference.

let us assume that the deviation from the straight line can be approximated by a second order polynomial. Under this mild assumption, Slater proposed to use the orbital energy at half charge to best approximate the total energy difference. Alternatively, under the same assumption, we proposed in Ref. 42 to approximate the total energy difference with the mean-value of the HOMO of the atom and the LUMO of the positive ion,

$$I \approx -\frac{\epsilon^{N}_{\mathrm{HOMO}} + \epsilon^{N-1}_{\mathrm{LUMO}}}{2}. \tag{24}$$

With this alternative evaluation of the ionization energy, there is no need to perform *GW* calculations for half charges. It requires nevertheless to perform two separate calculations. The outcome of the mean-value technique is given in Fig. 8 with the diamond symbols. For HF energies, the agreement between the mean-value and the ΔSCF energy difference is striking.

In the lower panel of Fig. 8, we compare the *GW* orbital energies to the RPA total energies. In this case, the HOMO energy of the atom is always slightly lower than the total energy difference, whereas the LUMO energy of the positive ion is always moderately higher. This proves the weak concavity of the *GW* approximations. Compared to HF, the *GW* orbital energies are much better estimates to the total energy difference. The associated localization error is then much weaker than the one of HF. The mean-value technique within *GW* yields a nice estimate of the RPA ΔSCF procedure. Only the end of the first row atom series deviates noticeably. This conclusion confirms our previous works on sodium clusters[42] on defects in solids[50,51] that first identified the slight concavity of the *GW* approximation. We confirm here that the mean-value technique is a more correct estimate to the total energy difference than the mere atom HOMO or cation LUMO.

VII. CONCLUSIONS

In this article, we described an implementation of the *GW* approximation to the electronic self-energy for atoms. This Gaussian basis set implementation does not need auxiliary functions and is based on an exact convolution in the frequency domain, so that no extra technical approximation is made besides the choice of the basis set. In addition to the usual perturbative approach to *GW* such as *GW*@LDA or *GW*@HF, we introduced the recently proposed self-consistent scheme named QS*GW*. The RPA correlation energies were obtained as a mere by-product of the code.

We considered different flavors of the *GW* approximation (*GW*@HF or QS*GW*) for the light atoms, from H to Ar. Noticeably, we calculated non-spherical atoms and spin-polarized systems, which have never been treated within *GW* to the best of our knowledge. An important technical conclusion of the present work is the slow convergence of the *GW* calculations with respect to the basis set size. This is however not completely surprising, when compared to RPA energy or MP2 energy convergence rates. The targeted error bar of 0.1 eV for HOMO/LUMO orbital energies could be reached only at the expense of a large cc-pV5Z basis set.

We then demonstrated the reliability of the *GW* approximation for the HOMO energy of atoms and for the LUMO energy of the cations compared to the experimental data. Since the HF approximation performs reasonably well for atoms and ions, the difference between perturbative *GW* based on HF (*GW*@HF) and self-consistent *GW* (QS*GW*) is not large, even though QS*GW* is slightly better on average. When turning to total energies, one could infer that the main ingredient missing in the RPA correlation is the second-order exchange diagram, which is contained in MP2. Comparing the total energy difference to the HOMO/LUMO orbital energy, we could confirm the weak concavity of the *GW* approximation for fractional electron numbers. The mean-value between the HOMO energy of the atom and the LUMO energy of the positive ion appears as a correct way to evaluate the total energy difference.

ACKNOWLEDGMENTS

We thank M. van Schilfgaarde and X. Blase for fruitful discussions and their comments on the manuscript.

[1] L. Hedin, Phys. Rev. **139**, A796 (1965).
[2] G. Strinati, H. J. Mattausch, and W. Hanke, Phys. Rev. B **25**, 2867 (1982).
[3] M. S. Hybertsen and S. G. Louie, Phys. Rev. B **34**, 5390 (1986).
[4] F. Aryasetiawan and O. Gunnarsson, Rep. Prog. Phys. **61**, 237 (1998).
[5] E. L. Shirley and R. M. Martin, Phys. Rev. B **47**, 15404 (1993).
[6] M. Rohlfing, Int. J. Quantum Chem. **80**, 807 (2000).
[7] A. Stan, N. E. Dahlen, and R. van Leeuwen, Europhys. Lett. **76**, 298 (2006).
[8] C. Rostgaard, K. W. Jacobsen, and K. S. Thygesen, Phys. Rev. B **81**, 085103 (2010).
[9] X. Blase, C. Attaccalite, and V. Olevano, Phys. Rev. B **83**, 115103 (2011).
[10] S.-H. Ke, Phys. Rev. B **84**, 205415 (2011).
[11] A. J. Cohen, P. Mori-Sánchez, and W. Yang, Science **321**, 792 (2008).
[12] J. C. Grossman, M. Rohlfing, L. Mitas, S. G. Louie, and M. L. Cohen, Phys. Rev. Lett. **86**, 472 (2001).
[13] F. Bruneval, N. Vast, L. Reining, M. Izquierdo, F. Sirotti, and N. Barrett, Phys. Rev. Lett. **97**, 267601 (2006).
[14] M. Gatti, F. Bruneval, V. Olevano, and L. Reining, Phys. Rev. Lett. **99**, 266402 (2007).
[15] H. Jiang, R. I. Gomez-Abal, P. Rinke, and M. Scheffler, Phys. Rev. B **82**, 045108 (2010).
[16] B. Holm and U. von Barth, Phys. Rev. B **57**, 2108 (1998).
[17] W. Ku and A. G. Eguiluz, Phys. Rev. Lett. **89**, 126401 (2002).
[18] A. Stan, N. E. Dahlen, and R. van Leeuwen, J. Chem. Phys. **130**, 114105 (2009).
[19] S. V. Faleev, M. van Schilfgaarde, and T. Kotani, Phys. Rev. Lett. **93**, 126406 (2004).
[20] F. Bruneval, N. Vast, and L. Reining, Phys. Rev. B **74**, 045102 (2006).
[21] M. van Schilfgaarde, T. Kotani, and S. Faleev, Phys. Rev. Lett. **96**, 226402 (2006).
[22] M. Shishkin, M. Marsman, and G. Kresse, Phys. Rev. Lett. **99**, 246403 (2007).
[23] C. Møller and M. S. Plesset, Phys. Rev. **46**, 618 (1934).
[24] G. Baym, Phys. Rev. **127**, 1391 (1962).
[25] N. E. Dahlen and U. v. Barth, Phys. Rev. B **69**, 195102 (2004).
[26] M. L. Tiago and J. R. Chelikowsky, Phys. Rev. B **73**, 205334 (2006).
[27] B. I. Lundqvist, Phys. Kondens. Mater. **6**, 206 (1967).
[28] H. N. Rojas, R. W. Godby, and R. J. Needs, Phys. Rev. Lett. **74**, 1827 (1995).
[29] T. H. Dunning Jr., J. Chem. Phys. **90**, 1007 (1989).
[30] D. Feller, J. Comp. Chem. **17**, 1571 (1996).
[31] K. Schuchardt, B. Didier, T. Elsethagen, L. Sun, V. Gurumoorthi, J. Chase, J. Li, and T. Windus, J. Chem. Inf. Model. **47**, 1045 (2007).
[32] See http://sourceforge.net/p/libint to obtain the library LIBINT, an efficient library for calculating the Coulomb integrals.
[33] M. E. Casida, *Recent Advances in Density Functional Methods, Part I* (World Scientific, Singapore, 1995), p. 155.

[34]F. Furche, J. Chem. Phys. **129**, 114105 (2008).
[35]A. Halkier, T. Helgaker, P. Jorgensen, W. Klopper, H. Koch, J. Olsen, and A. Wilson, Chem. Phys. Lett. **286**, 243 (1998).
[36]D. Foerster, P. Koval, and D. Sanchez-Portal, J. Chem. Phys. **135**, 074105 (2011).
[37]F. Furche, Phys. Rev. B **64**, 195120 (2001).
[38]E. C. Barnes and G. A. Petersson, J. Chem. Phys. **132**, 114111 (2010).
[39]*CRC Handbook of Chemistry and Physics*, 84th ed., edited by D. P. Lide (CRC, Boca Raton, Florida, 2003).
[40]W. Nelson, P. Bokes, P. Rinke, and R. W. Godby, Phys. Rev. A **75**, 032505 (2007).
[41]A. J. Morris, M. Stankovski, K. T. Delaney, P. Rinke, P. García-González, and R. W. Godby, Phys. Rev. B **76**, 155106 (2007).
[42]F. Bruneval, Phys. Rev. Lett. **103**, 176403 (2009).
[43]J. P. Perdew, R. G. Parr, M. Levy, and J. L. Balduz Jr., Phys. Rev. Lett. **49**, 1691 (1982).
[44]W. T. Yang, Y. Zhang, and P. W. Ayers, Phys. Rev. Lett. **84**, 5172 (2000).
[45]M. Grüning, A. Marini, and A. Rubio, J. Chem. Phys. **124**, 154108 (2006).
[46]F. Bruneval, F. Sottile, V. Olevano, and L. Reining, J. Chem. Phys. **124**, 144113 (2006).
[47]P. Mori-Sánchez, A. J. Cohen, and W. T. Yang, Phys. Rev. Lett. **100**, 146401 (2008).
[48]A. J. Cohen, P. Mori-Sánchez, and W. Yang, J. Chem. Theory Comput. **5**, 786 (2009).
[49]J. C. Slater, *The Self-Consistent Field for Molecules and Solids* (McGraw-Hill, New York, 1974), Vol. 4.
[50]M. Giantomassi, M. Stankovski, R. Shaltaf, M. Grüning, F. Bruneval, P. Rinke, and G.-M. Rignanese, Phys. Status Solidi B **248**, 275 (2011).
[51]F. Bruneval, Nucl. Instrum. Methods Phys. Res. B **277**, 77 (2012).